Tetrahedron 67 (2011) 7358–7369

Contents lists available at ScienceDirect

Tetrahedron

journal homepage: www.elsevier.com/locate/tet

Columnar/smectic metallomesogens derived from heterocyclic benzoxazoles

I-Tzu Wu [a], Pei-Yi Chaing [a], Wen-Jung Chang [a], Hwo-Shuenn Sheu [b], Gene-Hsiang Lee [c], Chung K. Lai [a,*]

[a] Department of Chemistry, National Central University and Center for Nano Science Technology, UST, Chung-Li, 32054, Taiwan, ROC
[b] National Synchrotron Radiation Research Centre, Hsinchu 30077, Taiwan, ROC
[c] Instrumentation Center, National Taiwan University, Taipei 10660, Taiwan, ROC

ARTICLE INFO

Article history:
Received 18 April 2011
Received in revised form 28 June 2011
Accepted 12 July 2011
Available online 4 August 2011

ABSTRACT

The synthesis, mesomorphic behavior, and optical properties of two new series of metal complexes **1a**,**b**–**M** (M=Pd, Cu, Zn) derived from benzoxazoles **2a**,**b** are reported. The crystal and molecular structures of mesogenic 5-decyloxy-2-(6-decyloxybenzooxazol-2-yl)phenol and nonmesogenic bis[5-octyloxy-2-(6-octyloxybenzooxazol-2-yl) phenol]Pd(II) were determined by means of X-ray structural analysis. Two benzoxazoles **2a** exhibited monotropic SmA phases, and all benzoxazoles **2b** were non-mesogenic. On the other hand, metal complexes **1a**–**M** exhibited distinctly different mesomorphism from complexes **1b**–**M**. Complexes **1a**–**Pd** formed SmC phases; complexes **1a**–**Cu** and **1a**–**Zn** formed crystal phases. In contrast, complexes **1b**–**Zn** exhibited columnar phases, and complexes **1b**–**Cu** and **1b**–**Pd** were nonmesogenic. The difference of the mesomorphism in **1a**–**M** and **1b**–**M** was probably attributed to the geometry and/or the overall molecular shape created by **2a** and **2b**. The electronic configuration of metal ion might play an important role in forming the mesophases. The fluorescent properties of these compounds were also examined.

1. Introduction

Coordination transition metal complexes, particularly for 3d-metals constitute the largest group among metallomesogenic materials.[1] Transition metal ions often have a variety of oxidation states and coordination numbers, therefore, numerous metal complexes with unique structures and physical properties can be expected. In fact, many metallomesogenic materials were obtained from nonmesogenic organic moieties. Zinc metal, as a late transition element constructed a major category of coordination compounds, which are essentially important in catalytic chemistry.[2] The importance stems from their chemical stabilities, versatile structures, and interesting photophysical behavior. A coordination number (CN) of four is more common over six for Zn^{2+} ion. Zinc ion prefers to coordinate both with bidentate ligands (η^2-L) and monodentate ligands (η^1-L), and resulting complexes formulated as neutral $Zn(\eta^2\text{-L})_2$, $Zn(\eta^2\text{-L})Cl_2$ or $Zn(\eta^1\text{-L})_2Cl_2$ were then obtained. In most of zinc complexes, both tetrahedral (T_d) and square planar (SP) geometries at central Zn^{2+} were often obtained. In general, metallomesogens incorporated with a square planar metal ion as core were better induced than those of a tetrahedral one due to its easier packing in crystal states or liquid crystal states. Zinc ion with a diamagnetic d^{10}-configuration has been applied to generate metallomesogens (i.e., metal-containing liquid crystals) during the past decades. Most of such known mesogenic zinc complexes were mainly derived from a various types of macrocyclic compounds, which included, such as phthalocyanines (Pcs),[3] porphrins,[4] tetrabenzoporphine,[5] and porphycenes.[6] Macrocyclic motifs are well known for their planar structures, rich conjugated π–electrons, thermal/photochemical stability, and high polarizability, which are better induced for the construction of mesogens and metallomesogens. In these metallomesogenic systems, a preferred bonding fashion of $[N_2N_2]$-donor atoms was often found. Such type of macrocyclic compounds and/or their transition metal complexes when substituted with linear or branched alkyl or alkoxy chains usually formed a major class of disc-like LCs, in which strong intermolecular π–π interactions were attributed to the formation of mesophases. In contrast, mesogenic zinc complexes derived from other mono-/bidentate ligands, such as salicyldimines,[7] 2,2′-bipyridines,[8] triazoles,[9] pyrazoles,[10] dipyrins,[11] oxazolines,[12] tropolones,[13] bilinones,[14] and imidazoles[15] were also known. In these examples, a bonding fashion of $[N_2O_2]$ and $[O_2O_2]$ was preferred. Incorporation of a Zn^{2+} ion into macrocycles led to square planar complexes, whereas, other monodentate (η^1-) or bidentate (η^2-) structures gave more likely slightly square planar or tetrahedral complexes. In contrast, a few mesogenic zinc complexes with a five-coordinated geometry[8b,16] were as well reported, and a distorted trigonal bipyramid geometry (TBP) made of three nitrogen atoms and two oxygen atoms $[N_3O_2]$ at central Zn^{2+} was obtained. Nematic phases, layered structures with smectic phases[17] or two-

* Corresponding author. Tel.: +886 03 4259207; fax: +886 03 4277972; e-mail address: cklai@cc.ncu.edu.tw (C.K. Lai).

0040-4020/$ – see front matter © 2011 Elsevier Ltd. All rights reserved.
doi:10.1016/j.tet.2011.07.024

dimensional columnar phases[16b,18] were commonly observed. Zinc complexes exhibiting lyotropic mesomorphism[19] was less observed. Zinc complexes based on heterocyclic derivatives also showed interesting optical properties. Mesogenic zinc complexes as well as other metal complexes, such as Lanthanides, Ni/Pd/Pt and Cu/Ag/Au complexes were considered as so-called luminescent metallomesogens.[18d,20]

Known metallomesogens derived from heterocyclic benzoxazoles[21,22] were relatively limited. A few known examples **I**–**II** were prepared and studied by this group.[22] Benzoxazoles, as well as other heterocycles, such as oxadiazoles, benzoxale, and oxazoles were found to exhibit interesting fluorescent properties[21] and their luminescent behavior were much affected substituent and/or conjugation length. In this paper, we describe syntheses and mesomorphic studies of two series of metallomesogens **1a**,**b** derived from benzoxazoles **2a**,**b** exhibiting smectic A or hexagonal columnar phases. Three metal ions, Pd^{2+}, Cu^{2+}, and Zn^{2+} were incorporated to understand the effect of the central geometry on the formation of mesophases. Complexes **1a**–**Pd** formed monotropic smectic C phases, whereas, all complexes **1a**–**Cu** and **1a**–**Zn** formed crystal phases. In contrast, complexes **1b**–**Zn** exhibited hexagonal columnar phases (Col_h), and all complexes **1b**–**Cu** and **1b**–**Pd** were nonmesogenic. The difference of the mesomorphic properties in compounds **1a**–**M** and **1b**–**M** was probably attributed to the geometry at metal center. The d^8-Pd^{2+} and d^{10}-Zn^{2+} ions are all diamagnetic, while d^9-Cu^{2+} ion is paramagnetic. The electronic configuration of metal ion might also play an important role in forming mesophase in such electron-deficient heterocyclic compounds. This is the first columnar zinc mesogens derived from benzoxazoles.

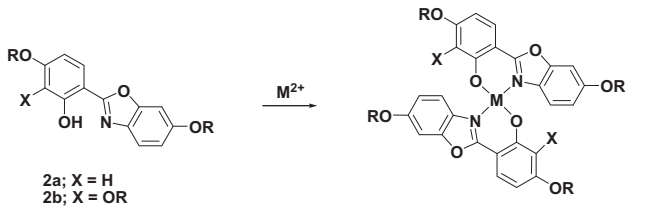

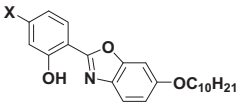

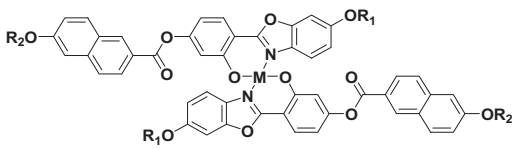

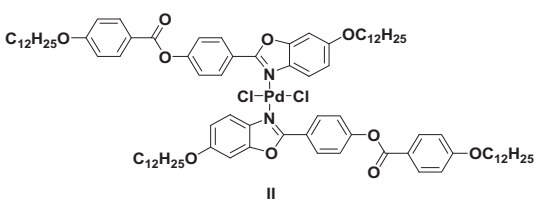

2. Results and discussion

2.1. Synthesis and characterization

The synthetic routes used to prepare benzoxazoles **2a**,**b** and their metal complexes **1a**–**M** and **1b**–**M** were summarized in Scheme 1. All synthetic procedures were similarly followed by literatures.[22] The final compounds **2a**,**b** were prepared by intracyclic reaction of intermediates **3a**,**b** with lead acetate $Pb(OAc)_4$ in $CHCl_3$ with a yield ranged from 78 to 90%. A singlet peak appeared at δ 8.49–8.51 ppm on ^1H NMR spectra is characteristically observed for imine–H (–C=NH–) group of compounds **3a**,**b**, and this peak was then disappeared upon formation of final products **2a**,**b**.The metal complexes were obtained by the reactions of appropriate benzoxazoles **2a**,**b** and copper(II), zinc(II) or palladium(II) acetate in refluxing THF/ethanol. Copper, zinc, and palladium complexes were isolated as a dark-green, off-white and light-yellow compounds. ^1H and ^{13}C NMR spectroscopy were used to characterize all intermediates, and the elemental analysis was used to confirm the purity of the metal complexes.

2.2. Single crystal structures of 5-decyloxy-2-(6-decyloxybenzooxazol-2-yl)phenol (2a; $n=10$) and bis[5-octyloxy-2-(6-octyloxybenzooxazol-2-yl)phenol]Pd(II) (1a–Pd; $n=8$)

In order to understand toe possible correlation between the molecular arrangements and mesomorphic behavior, two single crystals of the mesogenic benzoxazole **2a** (n=10) and non-mesogenic palladium complex **1a**–**Pd** (n=8) suitable for crystallographic analysis were obtained by slow diffusion from CH_2Cl_2/EtOH at room temperature and their structures resolved. Fig. 1 shows the two molecular structures with the atomic numbering schemes. Table 1 lists their crystallographic and structural refinement data for the molecules. Compound **2a** (n=10) crystallizes in a triclinic space group $P\bar{1}$ with a Z=2. The overall molecular shape of crystal **2a** (n=10) was considered as a linear structure with an overall molecular length of ~35.8 Å. The benzoxazole and central phenolic rings were nearly coplanar (dihedral angle=0.645°), however, they were not coplanar with the phenyl ring. As expected, an *intramolecular* H-bond between phenolic N1–H2 atoms was observed, and the distance was measured by ca. 1.890 Å. This near coplanarity of two rings was also observed in our other similar structures. The H-bonding kept the two rings close to coplanar, and the planar structure was responsible for a better packing both in the solid or/and the liquid crystal state. In the unit cell, all molecules were arranged by antiparallel and head-to-tail arrangements, shown in Fig. 2. A π–π interaction with a d ~3.65 Å (offset face to face alignment) is observed. No *intermolecular* H-bonding was formed, which was probably attributed to a quite short range of mesophase temperature in compounds **2a**.

In contrast, the palladium complex **1a** (n=8) also crystallizes in triclinic space group $P\bar{1}$ with a Z=1. The geometry at palladium center was coordinated as nearly perfect square planar. The two angles of N1–Pd1–O1 and N1A–Pd1-O1 atoms were of 91.248 (114)° and 88.752 (114)°, which were close to an angle of 90 expected for a perfect square planar geometry. The overall molecular shape was considered as lath-like with a length of ca. 33.97 Å. The two central planes defined by atoms Pd1–N1–C15–C16–O1 and Pd1–N1A–C15A–C16A–C21A–O1A atoms were perfectly coplanar with a dihedral angle of 0.000 (74)°. In the unit cell, two molecules were attracted with a weak π–π interaction. A distance, ~3.500 Å of point-to-face alignment between the phenyl ring C16–C21 and H2A and C16A–C21A and H2 was obtained. All alkoxy chains were interdigitated and the Van der Waal interaction between the alkoxy chains was observed. Also a weak interaction

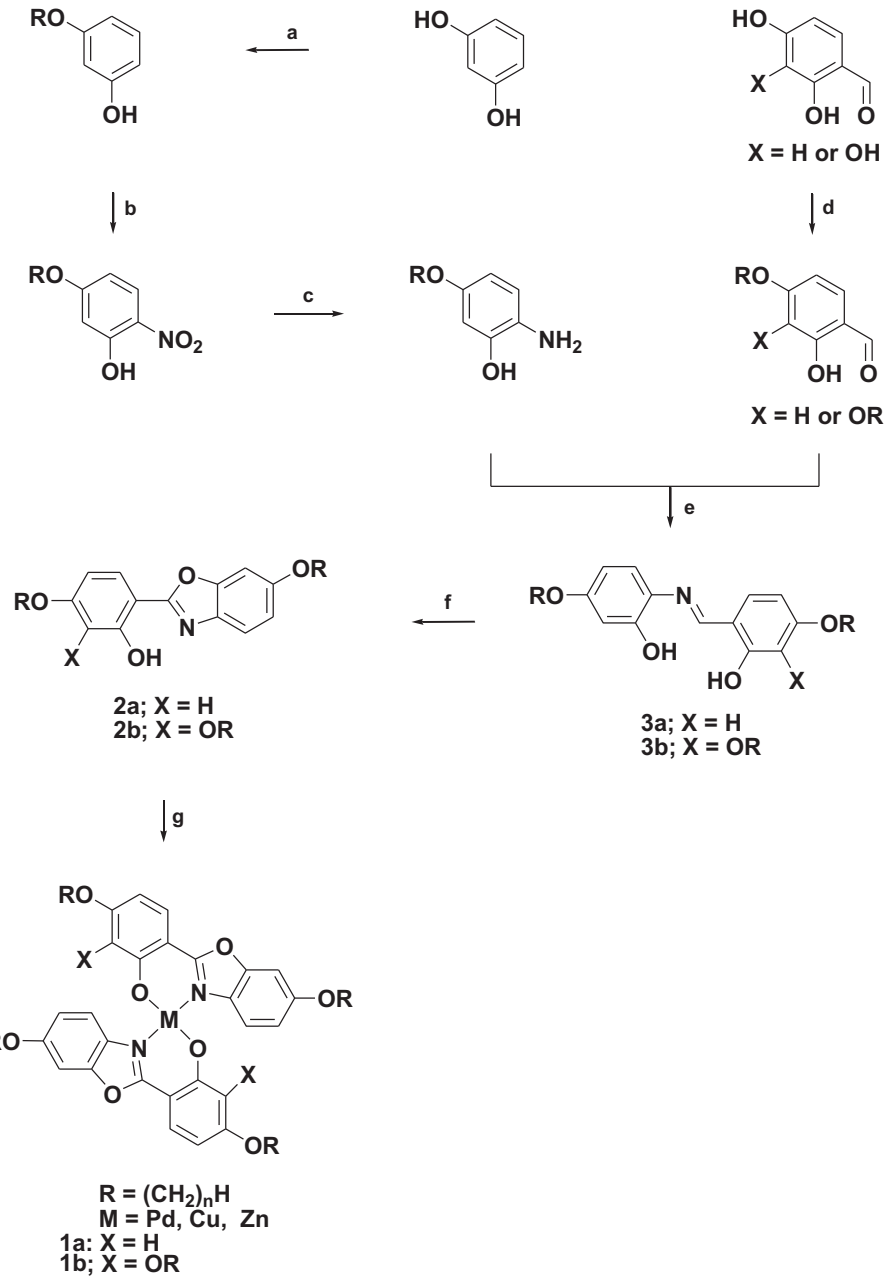

Scheme 1. Reactions and Reagents. a. RBr (1.1 equiv), $KHCO_3$ (1.5 equiv), refluxing in acetone, 24 h, 62–68%. b. HNO_3 (1.2 equiv), $NaNO_2$ (0.20 equiv), stirred at 0° C in CH_2Cl_2, 6 h, 25%. c. H_2NNH_2 (1.20 equiv), Pd/C (0.10 equiv), refluxing in C_2H_5OH, 4 h, 75–88% d. RBr (1.1 or 2.10 equiv), $KHCO_3$ (2.50 equiv), refluxing in acetone, 48 h, 38–62%. e. Acetic acid (drops), refluxing in C_2H_5OH, 24 h, 81–90%. f. $Pb(OAc)_4$ (1.10 equiv), refluxing in $CHCl_3$, 4 h, 78–90%. g. $M(OAc)_2$ (1.10 equiv), refluxing in THF/C_2H_5OH, 20 h, 88–92%.

between the O3–H14A and O3A–H14 with a distance of 3.0851 (29) Å was found. A layered structure for **2a** and **1a**–**Pd** was observed and the molecular arrangement in unit cell was also shown in Fig. 3.

2.3. Mesomorphic properties of benzoxazoles 2a,b

The liquid crystalline behavior of benzoxazole derivatives **2a**,**b** and their copper, zinc and palladium complexes **1a**–**M** and **1b**–**M** was investigated and studied by differential scanning calorimeter (DSC) and polarizing optical microscope (POM). The phase transitions and thermodynamic data of compounds **2a**,**b** were summarized in Table 2. Compounds **2a** formed mesomorphic behavior only for two derivatives n=10 and 12, while all others (n=8, 14, 16) were not mesogenic. The phases were monotropic, which indicated that the mesophases were kinetically unstable. All clearing or melting temperatures increased with carbon length, indicating that the van der Waals interaction between alkoxy chains was important. The two mesogenic derivatives (n=10, 12) have a relatively short temperature range of mesophase on cooling process, ΔT=6.80 °C (n=10) ~11.7 °C (n=12). This type of mesophase dependence on the carbon length is quite common in rod-like mesogens. The mesophases were characterized as smectic A phases by optical microscope, as their textures shown in Fig. 4. On cooling process, typical focal-conic textures with some homeotropic domains were easily observed. Within the layers of a smectic A phase, the long axes of the molecules lie parallel to one another, their direction being normal to the plane of the layer. All molecules are free to rotate about their long axes, and the distribution within the layers is random. This result was also supported by crystallographic data

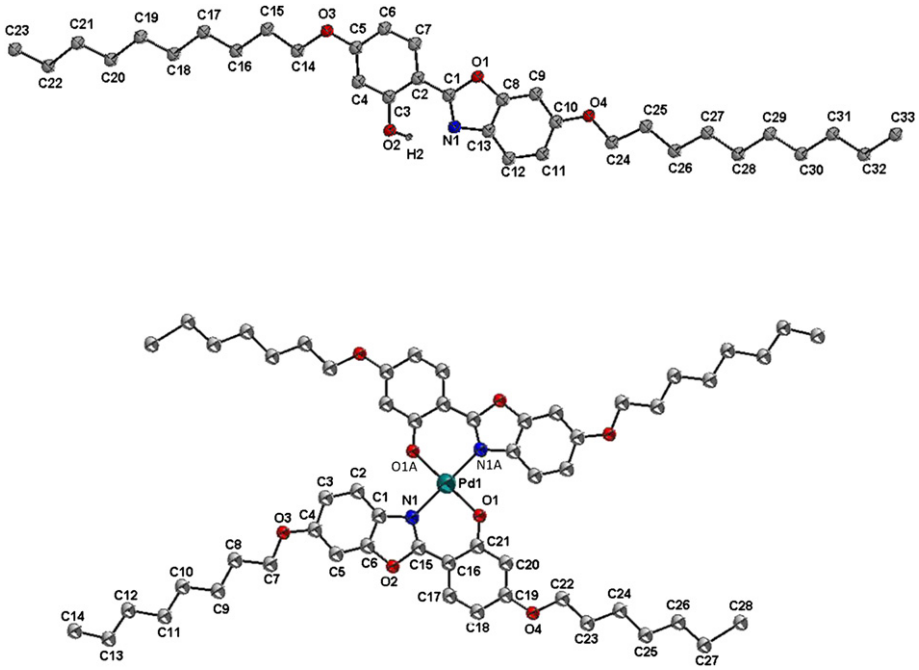

Fig. 1. Two ORTEP plots for **2a** (n=10; top) and **1a**–**Pd** (n=8) with the numbering scheme, and the thermal ellipsoids of the non-hydrogen are drawn at the 50% probability level. Selected bond lengths of **2a**; N1–C1, 1.3011 (21), O1–C1, 1.3811 (24), N1–C13, 1.4037 (24), O1–C8, 1.3814 (19), O2–H2, 0.8397 (12). Selected bond angles and bond lengths in **1a**–**Pd**: N1–Pd1–O1, 91.248 (114)°; O1–Pd1–N1A. 88.752 (114)°; N1A–Pd1–O1A, 91.248 (114)°; O1A–Pd1–N1, 88.752 (114)°; Pd1–N1, 2.0348 (27); Pd1–O1, 1.9648 (24); Pd1–N1A, 2.0348 (27); Pd1–O1A, 1.9648 (24).

Table 1
Crystallographic and experimental data for compound **2a** and **1a**–**Pd**

Compound	**2a** (n=10)	**1a**–**Pd** (n=8)
Empirical formula	$C_{33}H_{49}NO_4$	$C_{56}H_{74}N_2O_8Pd$
Formula weight	523.73	1009.57
T/K	100 (2)	293 (2)
Crystal system	Triclinic	Triclinic
Space group	P–1	P–1
a/Å	6.7337 (3)	5.5372 (2)
b/Å	12.2682 (4)	14.3557 (5)
c/Å	19.2682 (7)	18.2610 (6)
α/°	106.2964 (15)	73.437 (2)
β/°	97.5945 (16)	84.119 (2)
γ/°	93.7590 (16)	88.383
U/Å^3	1505.56 (10)	1384.02 (8)
Z	2	1
F(000)	572	534
D_c/Mg m^{-3}	1.155	1.211
Crystal size/mm^3	0.40×0.25×0.10	0.33×0.13×0.04
Range for data collection/°	1.11–25.00	1.17–28.43
Reflection collected	16,988	24,588
Data, restraints, parameters	5236/0/346	6862/0/306
Independent reflection	5236 [R(int)=0.0550]	6862 [R(int)=0.0310]
Final R_1, wR_2	R_1=0.0490, 0.1134	R_1=0.0536, 0.1435

discussed above. The crystallographic data indicated that all molecules were in fact antiparallel arranged (head-to-tail arrangement) between the neighboring layers. The benzoxazole was relatively considered as a larger electron-deficient core, and generally more extended terminal chains were required to induce the phase. Also in order to understand the effect of the polar groups on the formation of the mesophase, three derivatives **2c** (X=OCH_3, F, Cl) with a polar group substituted on the opposite end of the benzoxazole were also studied. The $-OCH_3$, –F, and –Cl groups were considered as strong π-donors and also electron-withdrawing groups. However, their mesomorphic properties were not improved. Only a crystal-to-isotropic transition was observed at T_{cl}=83.8 °C, 65.3 °C and 65.9 °C for derivatives X=$-OCH_3$, –F and –Cl. In contrast, all compounds **2b** (n=8, 12, 16) substituted with two more flexible terminal chains were nonmesogenic. A crystal-to-isotropic transition (Cr→I) with a larger enthalpy was all observed. The lack of mesomorphism was probably attributed to the shape effect. The overall molecular shape of compounds **2b** was considered as a lath-like, between rod-like and disc-like molecules, which might not facilitate the formation of the mesophases.

2.4. Mesomorphic properties of compound 1a,b

In order to understand the effect of the metal ion incorporated on the formation of the mesomorphic properties, a variety of complexes Cu^{2+}, Pd^{2+} and Zn^{2+} were prepared and studied. All metal complexes of **1a**–**M** with four alkoxy chains are more rod-like molecules, while metal complexes **1b**–**M** with six alkoxy chains are more likely disc-like molecules. The Pd^{2+} and Zn^{2+} ions are d^8- and d^{10}-diamagnetic, while Cu^{2+} ion is d^9-paramagnetic. Pd^{2+} ion prefers a square planar geometry. Meanwhile, Pd^{2+} or Cu^{2+} ion prefers a square planar or a slightly square planar geometry, and Zn^{2+} ion favors only a tetrahedral geometry.

The phase transitions and thermodynamic data of metal complexes **1a**–**M** and **1b**–**M** were summarized in Table 3. Complexes **1a**–**Pd** (n=10, 12, 14) are mesogenic, showing monotropic properties. On the other hand, both complexes **1a**–**Cu** and **1a**–**Zn** were not mesogennic. The clearing temperatures of three metal complexes **1a**–**M** were all higher than their precursor compounds **1a** as expected, by a ΔT_{cl}=40.9 °C (n=16)–86.7 °C (n=8) for **1a**–**Pd**, ΔT_{cl}=40.2 °C (n=16)–94.6 °C (n=8) for **1a**–**Cu** and ΔT_{cl}=26.8 °C (n=16)–109.3 °C (n=8) for **1a**–**Cu**. This was attributed to the larger molecular size or/and a more rigid core. All complexes **1a**–**Pd** (n=10, 12, 14) except two derivatives (n=8, 16) exhibited mesomorphic behavior. The clearing temperature decreased slightly with the terminal carbon length; by T_{cl}=154.2 °C (n=8)>136.2 °C (n=12)>129.1 °C (n=16). The influence of terminal alkoxy chains was not apparent in **1a**–**Pd**. Alkoxy chain lengths often has a more influence on the formation of rod-like liquid crystals; shorter chains prefer nematic and/or smectic A phase, while longer chains length form smectic C and/or higher Smectic X phase. An intermolecular interaction enhanced by van der Waals force of

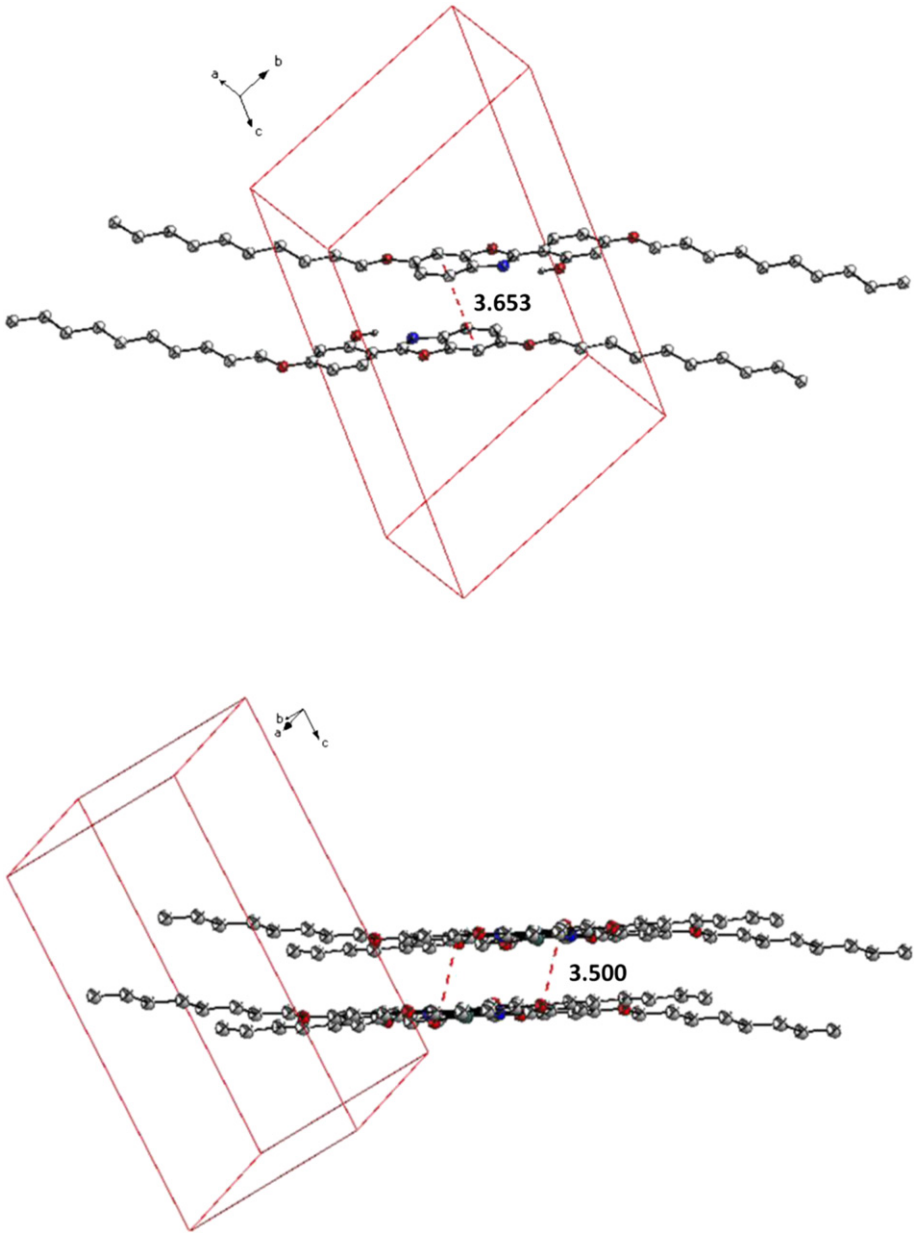

Fig. 2. The π–π interactions observed in the unit cell of **2a** (top) and **1a**–**Pd** (bottom).

alkoxy chains increases the interdigitation of alkoxy chains, often leading to a higher order of mesophases observed (Cr→N→SmA→SmC→SmX). The phases were identified and confirmed as smectic C phases by polarized microscope, and typical optical schlieren textures, shown in Fig. 5 were observed when cooling from isotropic states. The temperature range was relatively short, ΔT_{SmC}=7.8 °C (n=8), ~7.9 °C (n=12), and ~4.7 °C (n=14). The monotropic behavior and their shorter temperature ranges also indicated that the mesophases were kinetically unstable. A few other benzoxazoles and metal complexes **I** were previously reported in this group; palladium complexes also formed a relatively short temperature range (ΔTn=8.3–39.8 °C). In general, in order for a rod-like molecule to form nematic, SmA or/and SmC phase, an appropriate aspect ratio (d/l) is often needed. All these Pd complexes are not truly rod-like, but a lathe-like molecule. However, all complexes **1a**–**Cu** and **1a**–**Zn** complexes were not liquid crystals. A transition of crystal-to-isotropic was only observed, for example; T_{cl}=162.1 °C and T_{cl}=176.8 °C for **1a**–**Cu** (n=8) and **1a**–**Zn** (n=8), respectively. The clearing temperatures for complexes **1a**–**Cu** and **1a**–**Zn** decreased with carbon lengths; T_{cl}=162.1 °C (n=8)> 140.0 °C (n=12)>128.4 °C (n=16) for **1a**–**Cu** and T_{cl}=176.8 °C (n=8)>142.1 °C (n=12)>115.0 °C (n=16) for **1a**–**Zn** (n=8). The **1a**–**Zn** has a slightly higher clearing temperature than that of **1a**–**Cu**, indicating that the intermolecular force is *stronger* in **1a**–**Zn** than **1a**–**Cu**. Zinc complexes often have tetrahedral geometries, while copper complexes have slightly square planar or square planar geometries for such bidentate ligands as benzoxazoles.

Interestingly, metal complexes **1b**–**M** showed distinctly different mesomorphic properties from metal complexes **1a**–**M**. All complexes **1b**–**Zn** exhibited hexagonal columnar phase (Col_h) and other complexes **1b**–**Cu** and complexes **1b**–**Pd** formed crystal phases. Compounds **2b** have an extra alkoxy chains, giving to a total number of six alkoxy chains for complexes **1b**–**M**. For complexes **1b**–**Zn**, the DSC analysis showed a typical columnar phase transition, crystal-to-columnar-to-isotropic (Cr→Col→I). All compounds

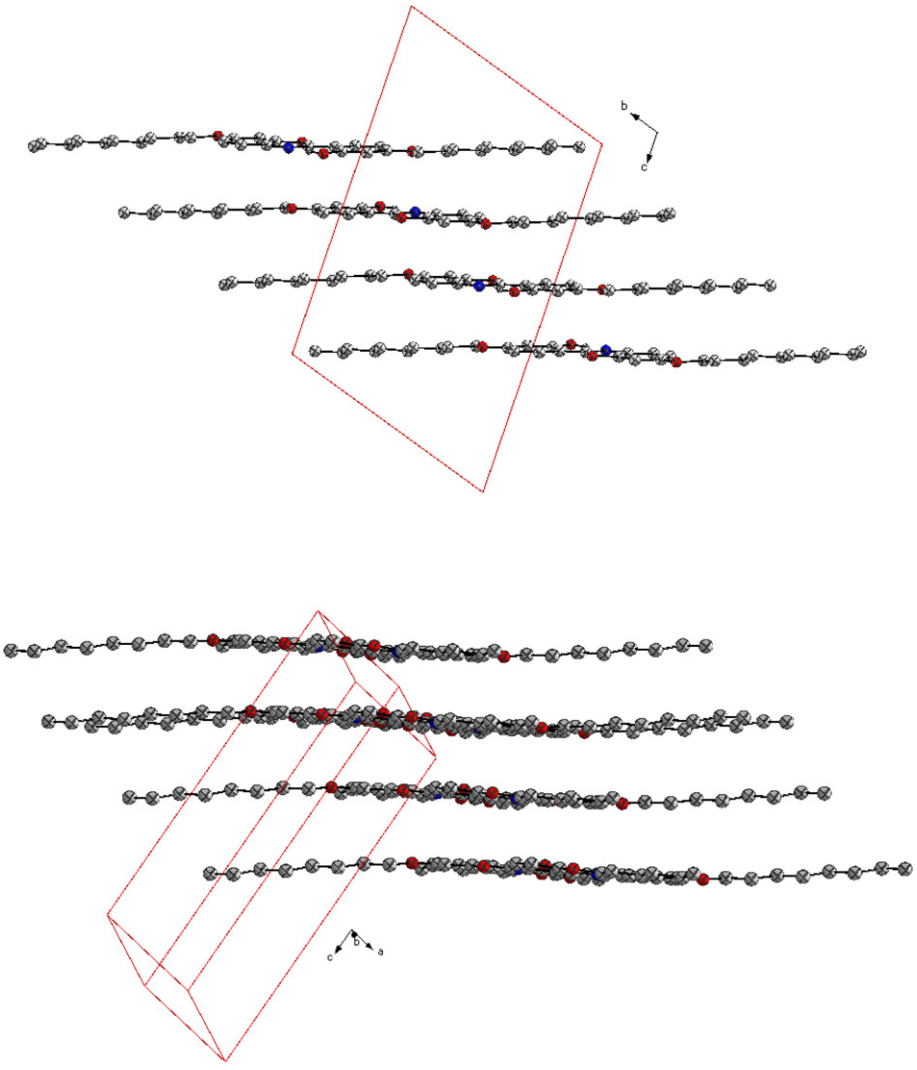

Fig. 3. The molecular arrangements for **2a** (top) and **1a**–**Pd** (bottom) in unit cell.

Table 2
Phase transitions and enthalpies[a] of compounds **2a**,**b**

2a; n = 8				**Cr**	$\underset{47.1\ (32.2)}{\overset{67.5\ (38.3)}{\rightleftharpoons}}$	**I**
10	**Cr**	$\underset{49.1\ (31.7)}{\overset{}{\rightleftharpoons}}$	**SmA**		$\underset{60.8\ (2.73)}{\overset{70.5\ (44.2)}{\rightleftharpoons}}$	**I**
12	**Cr**	$\underset{65.6\ (38.8)}{\overset{}{\rightleftharpoons}}$	**SmA**		$\underset{72.4\ (7.03)}{\overset{79.1\ (55.6)}{\rightleftharpoons}}$	**I**
14				**Cr**	$\underset{72.6\ (64.6)}{\overset{84.1\ (69.0)}{\rightleftharpoons}}$	**I**
16				**Cr**	$\underset{76.7\ (86.7)}{\overset{88.2\ (89.5)}{\rightleftharpoons}}$	**I**
2b; n = 8				**Cr**	$\underset{51.2\ (54.8)}{\overset{75.5\ (52.8)}{\rightleftharpoons}}$	**I**
12				**Cr**	$\underset{78.9\ (56.8)}{\overset{90.0\ (27.2)}{\rightleftharpoons}}$	**I**
16				**Cr**	$\underset{77.9\ (101)}{\overset{89.3\ (98.1)}{\rightleftharpoons}}$	**I**

[a] Phase transition temperature (°C) and enthalpies (KJ/mol) were determined by DSC at a scan rate of 20° C min^{-1}. Cr=crystalline, SmA=smetic A and I=isotropic phase.

1b–**Zn** (except for the shorter derivative n=8) exhibited enantiotropic behavior. The only complex with the shortest chain (n=8) was not mesogenic due to the insufficient chain flexibility. Both melting and clearing temperatures decreased with carbon chain length, T_{mp}=160.6 °C (n=10)>127.1 °C (n=16) and T_{cl}=163.9 °C (n=10)>142.0 °C (n=16). On the other hand, the temperature range of columnar phase stayed close to ΔT_{Col}=18.5 °C (n=8)–15.0 °C (n=12) on the cooling process. In addition, a smaller enthalpy (ΔH=3.23–6.03 kJ/mol on heating cycle) for the $Col_h \rightarrow$I transition was observed, indicating that the molecular order in the columnar phase was slightly ordered. The mesophase was first characterized by optical microscope. Under POM, for example, compound **1b**–**Zn** (n=12) displayed an optical texture of pseudo focal-conics with linear birefringent defects (Fig. 5), suggesting a columnar structure. A small area of homeotropic domains was also observed. In columnar mesophases, the disc-like molecules stack into columns in a hexagonal (Col_h) or rectangular (Col_r) superstructure. Within a column the molecules can be either periodically or aperiodically stacked. However, all complexes **1b**–**Cu** and **1b**–**Pd** were not mesogenic. A single transition from crystal phase to isotropic state (Cr→I) was obtained, at T_{cl}=117.5 °C and T_{cl}=136.2 °C for **1b**–**Cu** and **1b**–**Pd**, respectively. The observed mesomorphism was distinctly different from compounds **1a**–**M**. The lack of mesomorphic properties in this series of copper and palladium complexes might be attributed to the central geometry. Zinc ion often prefers

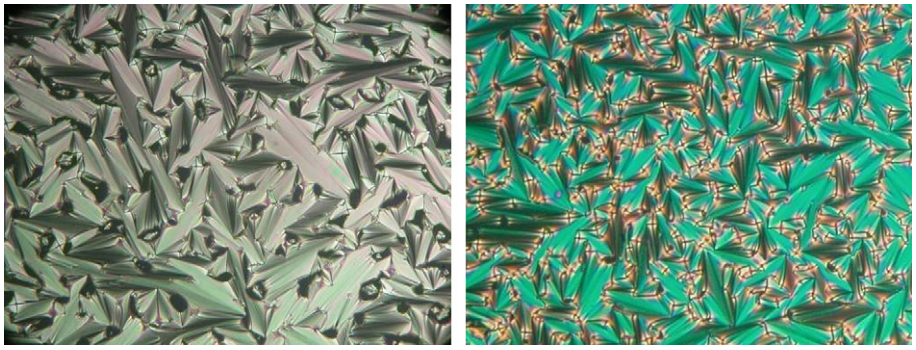

Fig. 4. The optical textures observed. SmA phase by **2a** (n=10; left) at 60 °C; SmA phase by **2a** (n=12; right) at 72 °C.

Table 3
Phase transitions and enthalpies[a] of compounds **1a**–**M** and **1b**–**M**

1a-Pd; n = 8			Cr	154.2 (39.7) / 132.4 (36.2)	I
10	Cr	110.6 (33.8)	SmC	140.9 (45.4) / 118.4 (10.7)	I
12	Cr	109.3 (40.8)	SmC	136.2 (57.2) / 117.2 (9.96)	I
14	Cr	105.7 (70.1)	SmC	130.3 (83.4) / 110.4 (11.2)	I
16			Cr	129.1 (95.0) / 109.7 (93.5)	I
1a-Cu; n = 8			Cr	162.1 (45.5) / 144.3 (44.6)	I
12	Cr_1	115.7 (13.7)	Cr_2	117.6 (14.9) / 140.0 (49.4) / 131.0 (48.6)	I
16	Cr_1	52.1 (22.8)	Cr_2	61.7 (27.9) / 128.4 (89.0) / 120.7 (83.4)	I
1a-Zn; n = 8			Cr	176.8 (22.4) / 150.6 (20.3)	I
12			Cr	142.1 (19.6) / 116.1 (16.3)	I
16	Cr_1	73.9 (13.4)	Cr_2	78.7 (14.5) / 115.0 (20.9) / 99.4 (18.0)	I
1b-Zn; n = 8			Cr	156.2 (8.26) / 137.6 (5.79)	I
10	Cr	142.2 (7.15)	Col_h	160.6 (3.87) / 163.9 (3.23) / 160.7 (6.01)	I
12	Cr	137.2 (3.47)	Col_h	153.0 (0.94) / 157.0 (3.26) / 152.0 (5.20)	I
14	Cr	128.3 (1.44)	Col_h	143.7 (5.54) / 152.4 (6.34) / 145.9 (5.03)	I
16	Cr	121.7 (1.60)	Col_h	127.1 (2.89) / 142.0 (4.18) / 137.9 (4.13)	I
1b-Cu; n = 10			Cr	117.5 (90.2) / 100.0 (94.2)	I
1b-Pd; n = 10			Cr	143.5 (108) / 133.5 (107)	I

[a] n is the carbon numbers in the alkoxy chains. Cr=crystal phase, SmC=smectic C and Col_r=rectangular columnar phase. The transition temperature (°C) and enthalpies (in parenthesis, KJ/mol) are determined by DSC analysis at a scan rate of 10.0 °C/min.

a tetrahedral geometry, while copper and palladium favors a slightly square planar or square planar geometry. The clearing temperatures of compounds **1b**–**M** were ranged in order of **1b**–**Zn**>**1b**–**Pd**>**1b**–**Cu**. The molecular interaction in **1b**–**Pd** and **1b**–**Cu** might not be strong enough for complexes **1b**–**Pd** and **1b**–**Cu** to be induced for the formation of the mesophases. However, the benzoxazole is often considered as an electron-deficient heterocycle. The electronic configuration of the central ions, d^9-Cu and d^8-Pd might be another important factor for the lack of any mesophase formed.

2.5. Powder X-ray diffraction of compounds 1b

Variable-temperature powder XRD diffraction experiments were conducted to confirm the structures of the mesophases of compounds **1b**–**Zn** (n=16). A typical diffraction pattern of a two-dimensional hexagonal lattice with one very strong diffraction peak at lower angle and two much weaker diffraction peaks was all observed. These are characteristic of hexagonal columnar phases with a d-spacing ratio of 1, $(1/3)^{1/2}$, and $(1/4)^{1/2}$, corresponding to Miller indices; 10, 11, and 20, respectively. For example, a diffraction pattern at 130 °C with a d-spacing at 28.2 Å, 16.3 Å, 14.1 Å and a broad diffuse peak (~4.71 Å) at wide-angle region was observed for compound **1b**–**Zn** (n=16) and this diffraction pattern corresponded to a hexagonal columnar arrangement (see Fig. 6). This diffraction pattern corresponds to an *inter*-columnar distance or lattice constant (i.e., a parameter of the hexagonal lattice) of a=32.6 Å. This lattice constant is slightly than the length of molecule calculated by MM2, indicating that the alkoxy chains might be slightly interdigitated. At lower nonmesogenic temperature (T=100 °C) the first peak moved to smaller angle (d ~29.3 Å). The presence of a relatively weak peak at wide angles (d ~3.60 Å) indicated that all molecules might be slightly ordered along the columns. However, liquid-like correlations between the rigid cores occurred at wide-angle regions of 4.71 Å. The hexagonal lattices were correlated well with side-chain alkoxy carbon lengths.

2.6. Optical properties

Heterocyclic benzoxazoles have been an excellent candidate as potential light emitting materials due to their photophysical and fluorescent properties. The luminescent properties observed by this type of heterocyclic molecules were often affected by polar substituents, position and/or conjugation length. 2-(2-Hydroxyphenyl) benzoxazole (HBO)[23] has been extensively studied due to its dual emission via the excited-state intramolecular proton transfer (ESIPT).[22] In contrast, known luminescent metallomesogens[20] were relatively rare. A few ions, particularly of d^8-Pd^{2+}/Pt^{2+}, d^{10}-Cu^+ and d^{10}-Zn^{2+} are in fact considered as promising ions to be potentially luminescent metallomesogens. Absorption and emission spectra of compounds **2a**,**b** (n=12), **1a**–**Zn** (n=12) and **1b**–**Zn** (n=12) measured in CH_2Cl_2 at 25 °C are shown in Fig. 7. The highest absorption peaks of all compounds were found to be insensitive to the carbon

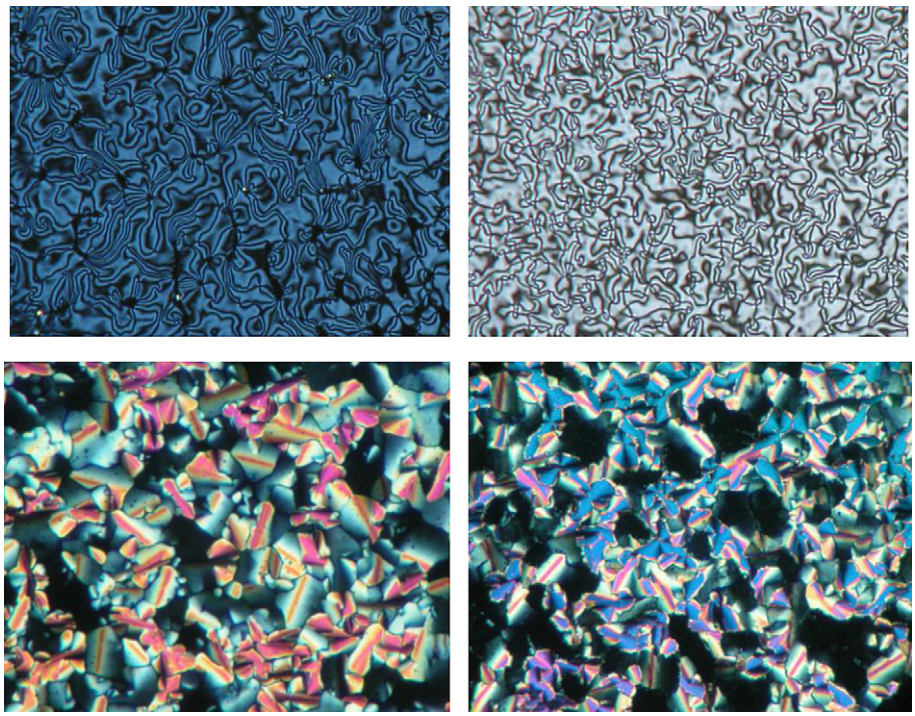

Fig. 5. The optical textures observed. SmC phase by **1a**–**Pd** (n=10; top left) at 112 °C, SmC phase by **1a**–**Pd** (n=12; top right) at 114 °C, **1b**–**Zn** (n=12; bottom left), and Col_h phase at 150 °C and Cr phase at 70 °C (bottom right).

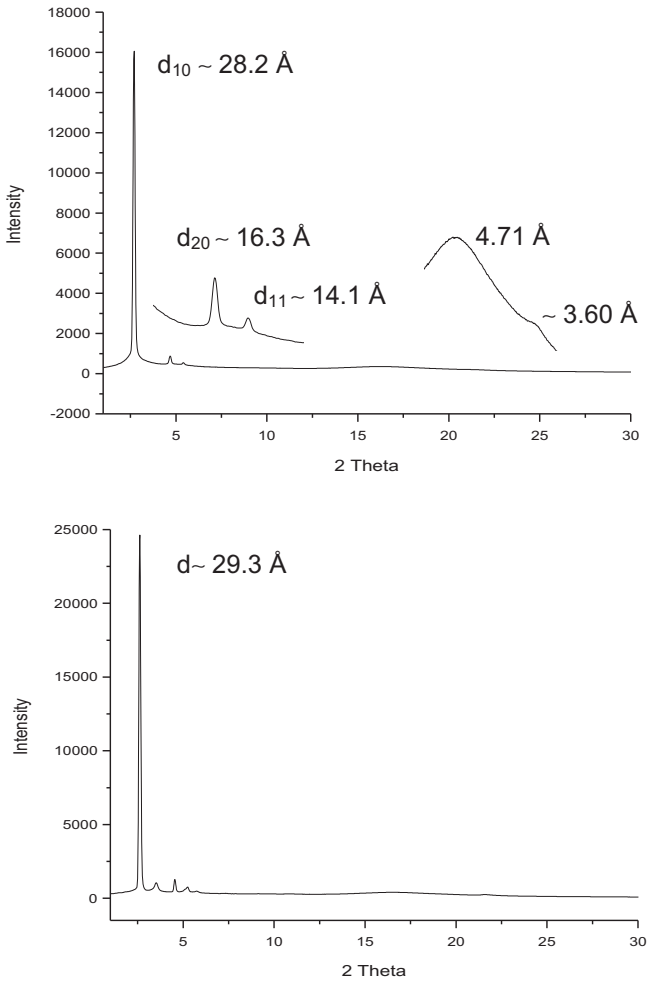

Fig. 6. The XRD diffraction plots for **1b**–**Zn** (n=16) at 130 °C (top) and at 100 °C (bottom).

length. Compounds **2a**,**b** showed two, low-energy π–π*; absorption at 328–329 nm (as λ_{max}) and 344–345 nm (see Table 4). The former band was assigned to the *anti*-enol, and the later band corresponded to the *syn*-enol. On the other hand, complexes **1a**–**Zn** and **1b**–**Zn** occurred at 328–329 nm (as λ_{max}) and 344–345 nm. The emission peaks for **2a** and **2b** occurred at 467.0 nm and 370.4 nm, while **1a**–**Zn** and **1b**–**Zn** occurred at 407.1 nm and 440.8 nm, respectively. Compound **2b** showed a blue-shift of ca. 96.6 nm over **2a** due to a promotion effect of ESIPT. Compound **2b** has a second alkoxy group substituted on *meta*-position to the benzoxazole ring. The fluorescence emission originates a π–π*; transition. The emission fluorescent spectra measured in different solvents and solid state were also studied. A slight shift, for example for **2a** (n=12) was observed; λ_{max}=466 nm as solid, 467 in CH_2Cl_2, 476 in hexane and 461 nm in ethanol. The emission wavelength in the solid state remained the same as that in CH_2Cl_2 with lower emission intensity. In general, benzoxazole, when measured in nonpolar solvent emitted long wavelength fluorescence exclusively via the ESIPT process of the excited state of the intramolecular hydrogen-bonded enol. On the other hand, compound **1b**–**Zn** showed a slight red-shift of ca. 33.7 nm over **1a**–**Zn**. The zinc complexes emit more intensity in the same spectral region than those of free ligands, and also, non-planar geometry at zinc(II) often prevents the formation of excimers.[20b] The quantum yields estimated with anthracene as a standard (φ_f=0.27 in hexane) were ranged from *ca.* 0.02–0.03% and 0.10–0.18% for **2a**,**b** and **1a**,**b**, respectively.

3. Conclusions

Two series of metallomesogens derived benzoxazoles **1a**,**b** were prepared and their mesomorphic properties studied. Compounds **2a** (n=10, 12) exhibited monotropic smectic A phases. Complexes **1b**–**M** exhibited distinctly different mesomorphism from complexes **1a**–**M**. Complexes **1a**–**Pd** (n=10, 12, 14) formed monotropic smectic C phases, whereas, all complexes **1a**–**Cu** and **1a**–**Zn** formed crystal phases. In contrast, complexes **1b**–**Zn** (n=10, 12, 14,

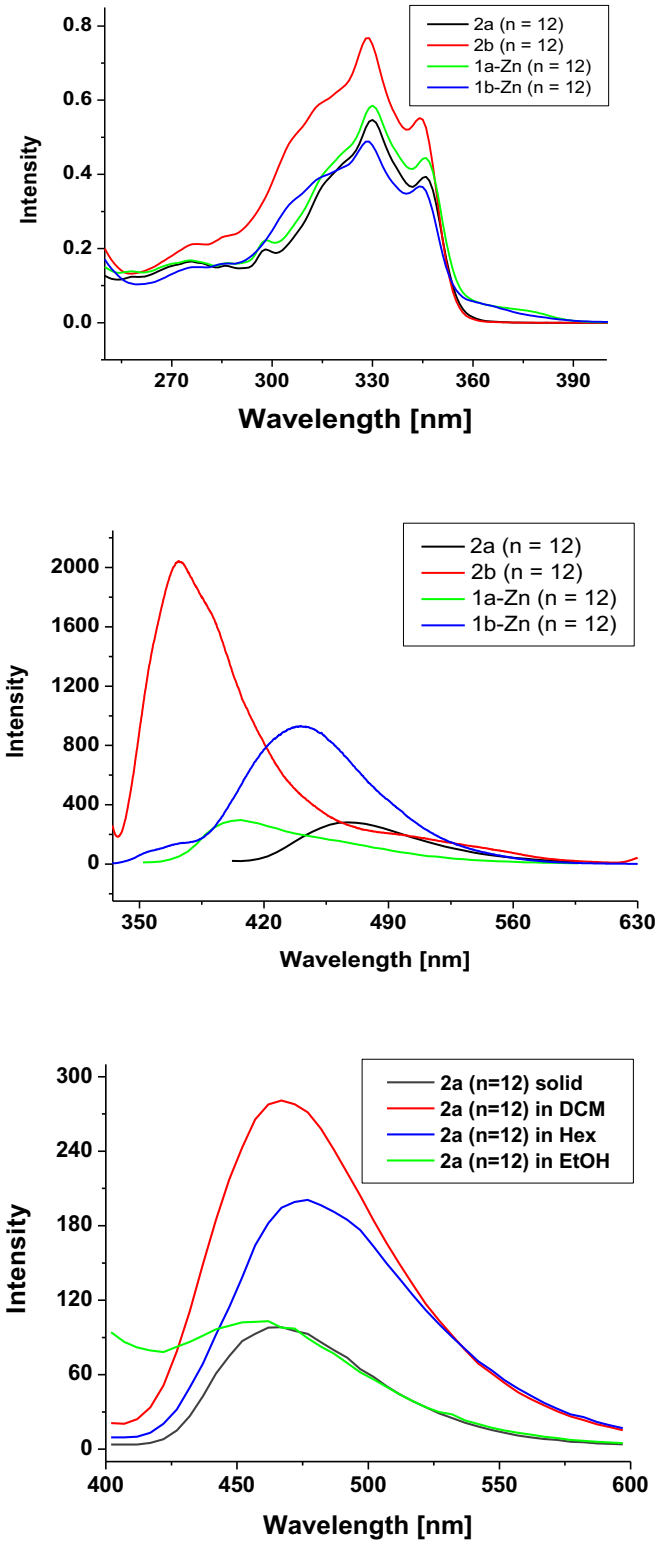

Fig. 7. UV (top) and PL spectra (center and bottom) of the compounds **2a**,**b**.

Table 4
A summary of UV and PL peaks[a] for compounds **2a**,**b** and **1a**,**b**–**Zn**

Compds	UV (nm)	PL (nm)
2a (n=12)	329 (λ_{max}), 319 (sh), 345	467.0
2b (n=12)	328 (λ_{max}), 314 (sh), 344	370.4
1a–**Zn** (n=12)	329 (λ_{max}), 320 (sh), 345	407.1
1b–**Zn** (n=12)	328 (λ_{max}), 313 (sh), 344	440.8

[a] Spectra measured in CH_2Cl_2 at rt.

16) exhibited hexagonal columnar phases, and all other complexes **1b**–**Cu** and **1b**–**Pd** were nonmesogenic. The difference of the mesomorphic properties in compounds **1a**–**M** and **1b**–**M** (M=Pd, Zn, Cu) was probably attributed to the geometry at metal center. Zinc(II) complexes **1a**,**b**–**Zn** emitted typical large luminescent bands originating from π–π^*; transitions, centered at ca. 407.1–440.8 nm in CH_2Cl_2 at room temperature, while palladium and copper complexes **1a**,**b**–**M** (M=Pd, Cu) were in fact non-emissive. The quantum yields were relatively lower.

4. Experimental section

4.1. General

All chemicals and solvents were reagent grades from Aldrich Chemical Co. Tetrahydrofuran (THF) was distillated from Na metal or CaH_2, and CH_2Cl_2 was distillated from P_2O_5. ^1H and ^{13}C NMR spectra were measured on a Bruker DRS-200. DSC thermographs were carried out on a Mettler DSC 822 and calibrated with a pure indium sample. All phase transitions are determined by a scan rate of 10.0 °C/min. Optical polarized microscopy was carried out on Zeiss Axioplan 2 equipped with a hot stage system of Mettler FP90/FP82HT. The UV–vis absorption and fluorescence spectra were obtained using a Jasco V-530 and Hitachi F-4500 spectrometer. All spectra were measured in $CHCl_3$ at room temperature, and the excitation wavelength of the fluorescent spectra was 397 nm. Elemental analyses were performed on a Heraeus CHN–O-Rapid elemental analyzer, and their mass spectra were also measured. The powder diffraction data were collected from the Wiggler-A beam line at National Synchrotron Radiation Research Center (NSRRC) with a wavelength of 1.3263 Å. Diffraction patterns were recorded in $\theta/2\theta$ geometry with step scans normally 0.02° in 2θ=1–10° step^{-1} s^{-1} and 0.05° in 2θ=10–5° step^{-1} s^{-1} and a gas flow heater was used to control the temperature. The powder samples were charged in Lindemann capillary tubes (1.00 mm) from Charles Supper. The synthetic procedures for compounds, 3-alkoxyphenols, 5-alkoxy-2-nitrophenols, 2-amino-5-alkoxy phenols, 4-alkoxyxy-2-hydroxybenzaldehydes, and 2-hydroxy-4-alkoxy-*N*-(2-hydroxy- 4-alkoxybenzylidene)anilines were followed by literatures.[24]

4.1.1. 3-Dodecyloxyphenol. White solid; yield 52%. ^1H NMR ($CDCl_3$): δ 0.86 (t, 3H, $-CH_3$, J=6.4 Hz), 1.25–1.40 (m, 18H, $-CH_2$), 1.67–1.78 (m, 2H, $-OCH_2CH_2$), 3.90 (t, 2H, $-OCH_2$, J=6.6 Hz), 6.39–6.49 (m, 3H, Ar–H), 7.10 (t, 1H, Ar–H, J=8.5 Hz). ^{13}C NMR ($CDCl_3$): δ 14.12, 22.68, 26.01, 29.19, 29.34, 29.38, 29.57, 29.63, 31.90, 68.02, 101.99, 107.00, 107.51, 130.05, 156.66, 160.48.

4.1.2. 5-Dodecyloxy-2-nitrophenol. Yellow solid; yield 42%. ^1H NMR ($CDCl_3$): δ 0.85 (t, 3H, $-CH_3$, J=6.3 Hz), 1.24–1.45 (m, 18H, $-CH_2$), 1.71–1.82 (m, 2H, $-OCH_2CH_2$), 3.99 (t, 2H, $-OCH_2$, J=6.5 Hz), 6.45–6.51 (m, 2H, Ar–H), 8.00 (d, 1H, Ar–H, J=10.1 Hz), 11.03 (s, 1H, Ar–OH). ^{13}C NMR ($CDCl_3$): δ 14.10, 22.66, 25.83, 28.79, 29.24, 29.32, 29.49, 29.54, 29.60, 31.88, 69.11, 101.73, 109.83, 114.54, 126.89, 157.99, 166.71.

4.1.3. 2-Amino-5-dodecyloxyphenol. Off-white solid; yield 86%. ^1H NMR ($CDCl_3$): 0.86 (t, J=6.7 Hz, $-CH_3$, 3H), 1.24–1.38 (m, $-CH_2$, 18H), 1.67–1.71 (m, $-OCH_2$, 2H), 3.84 (t, J=6.5 Hz, $-OCH_2$, 2H), 6.42–6.45 (d, J=7.6 Hz, –ArH, 2H), 6.74 (s, –ArH, 1H), 11.03(s, –OH, 1H). ^{13}C NMR ($CDCl_3$): 14.10, 23.12, 28.81, 29.25, 29.26, 29.32, 29.5, 29.49, 29.61, 31.91, 72.28, 102.17, 107.60, 117.23, 125.64, 144.53, 162.17. IR (neat): 3352, 3268 ($-NH_2$) cm^{-1}.

4.1.4. 4-Dodecyloxy-2-hydroxybenzaldehyde. White solid; yield 54%. ^1H NMR ($CDCl_3$): δ 0.86 (t, 3H, $-CH_3$, J=6.8 Hz), 1.24–1.43 (m,

18H, $-CH_2$), 1.74–1.84 (m, 2H, $-OCH_2CH_2$), 3.97 (t, 2H, $-OCH_2$, J=6.6 Hz), 6.38 (s, 1H, Ar–H), 6.49 (dd, 1H, Ar–H, J=1.8, 8.7 Hz), 7.38 (d, 1H, Ar–H, J=8.5 Hz), 9.67 (s, 1H, Ar–CHO), 11.45 (s, 1H, Ar–OH). ^{13}C NMR ($CDCl_3$): δ 14.12, 22.70, 25.93, 25.98, 26.06, 28.20, 28.79, 28.94, 29.32, 29.36, 29.46, 29.55, 29.56, 29.59, 29.64, 31.93, 32.87, 33.99, 68.61, 101.06, 108.76, 115.02, 135.17, 164.55, 166.47, 194.25.

*4.1.5. 2-Hydroxy-4-dodecyloxy-N-(2-hydroxy-4-dodecyloxybenzylidene)aniline (**3a**; n=12).* Light yellow solid; yield 78%. ^{1}H NMR ($CDCl_3$): δ 0.88 (t, 6H, $-CH_3$, J=6.9 Hz), 1.27–1.46 (m, 36H, $-CH_2$), 1.74–1.80 (m, 4H, $-OCH_2CH_2$), 3.94 (t, 2H, $-OCH_2$, J=6.6 Hz), 3.99 (t, 2H, $-OCH_2$, J=6.6 Hz), 6.47–6.50 (m, 3H, Ar–H), 6.56 (s, 1H, Ar–H), 7.04 (d, 1H, Ar–*H*, J=8.8 Hz), 7.24 (t, 1H, Ar–H, J=4.6 Hz), 8.51 (s, 1H, Ar–CH=*N*–Ar). ^{13}C NMR ($CDCl_3$): δ 13.92, 22.58, 25.94, 25.99, 29.06, 29.21, 29.24, 29.27, 29.31, 29.47, 29.50, 29.55, 29.57, 31.84, 68.38, 68.49, 101.73, 101.83, 107.68, 107.86, 113.37, 118.12, 129.19, 133.55, 150.95, 159.65, 160.51, 162.76, 163.69.

*4.1.6. 2-Hydroxy-4-dodecyloxy-N-(2-hydroxy-3, 4-didodecyloxybenzylidene)aniline (**3b**; n=12).* The mixture of 2-amino-5-dodecyloxyphenol (2.0 g, 6.82 mmol), 3,4-didodecanoxy-2-hydroxybenzaldehyde (2.8 g, 6.20 mmol) and a few drops of acetic acid was refluxed in 100 mL of absolute ethanol for 24 h under nitrogen atmosphere. The orange-brown crude product was collected. The product isolated as yellow-orange solids was obtained after recrystallization from CH_2Cl_2/hexane (1/1). Yield 85%. ^{1}H NMR ($CDCl_3$): δ 0.87 (t, 9H, $-CH_3$, J=6.9 Hz), 1.26–1.41 (m, 54H, $-CH_2$), 1.70–1.81 (m, 6H, $-OCH_2$), 3.90 (t, 2H, $-OCH_2$, J=6.50 Hz), 3.99–4.05 (m, 4H, $-OCH_2$), 6.42–6.60 (m, 3H, Ar–H), 7.04–7.09 (m, 2H, Ar–H), 8.49 (s, 1H, Ar–CH=N–Ar). ^{13}C NMR ($CDCl_3$): δ 14.09, 22.67, 26.02, 26.05, 29.34, 29.40, 29.57, 29.63, 31.90, 68.27, 68.76, 73.28, 101.65, 104.26, 107.44, 114.41, 117.88, 127.77, 135.98, 151.13, 156.26, 156.57, 159.30, 159.59. IR (neat): 2982, 2921, 2852, 1633, 1601, 1442, 1276, 1189, 1110, 922, 786 cm^{-1}.

*4.1.7. 5-Decyloxy-2-(6-decyloxybenzoxazol-2-yl)phenol (**2a**; n=12).* The solution of 2-decyloxy-4-decyloxy-*N*-(2-hydroxy-4-decyloxybenzylidene)aniline (1.00 g, 1.90 mmol) dissolved in 150 mL of $CHCl_3$ was added lead acetate (1.01 g, 2.30 mmol) under nitrogen atmosphere. The solution was gently refluxed for 4 h. The solution was concentrated under reduced pressure, and the residue was abstracted twice with CH_2Cl_2/H_2O (1/5). The organic layers were combined and dried over $MgSO_4$. The product was purified by passage to a short column of silica gel eluting with hexane/EA (1:1). The product isolated as white solids was obtained after recrystallization from CH_2Cl_2/CH_3OH. Yield 78–83%. ^{1}H NMR ($CDCl_3$): δ 0.85 (t, 6H, $-CH_3$, J=6.90 Hz), 1.25–1.45 (m, 28H, $-CH_2$), 1.74–1.81 (m, 4H, $-OCH_2CH_2$), 3.95–3.99 (m, 4H, $-OCH_2$), 6.50–6.57 (m, 2H, Ar–H), 6.90 (q, 1H, Ar–H, J=2.1 Hz), 7.05 (d, 1H, Ar–H, J=2.1 Hz), 7.49 (d, 1H, Ar–H, J=8.7 Hz), 7.81 (d, 1H, Ar–H, J=8.7 Hz). ^{13}C NMR ($CDCl_3$): δ 14.12, 22.69, 26.01, 26.06, 29.10, 29.24, 29.34, 29.39, 29.58, 31.91, 68.25, 68.92, 96.22, 101.66, 103.88, 107.96, 113.20, 118.63, 127.76, 133.72, 149.88, 157.52, 160.07, 162.31, 163.30. Anal. Calcd for $C_{33}H_{49}NO_4$: C, 75.68; H, 9.43; N, 2.67. Found C, 75.76; H, 9.44; N, 2.60.

*4.1.8. 5-Octyloxy-2-(6-octyloxybenzoxazol-2-yl)phenol (**2a**; n=8).* White solid; yield 72%. ^{1}H NMR ($CDCl_3$): δ 0.86 (t, 6H, $-CH_3$, J=6.9 Hz), 1.27–1.52 (m, 20H, $-CH_2$), 1.75–1.82 (m, 4H, $-OCH_2CH_2$), 3.95–4.00 (m, 4H, $-OCH_2$), 6.50–6.57 (m, 2H, Ar–H), 6.90 (q, 1H, Ar–H, J=2.4 Hz), 7.06 (d, 1H, Ar–H, J=2.1 Hz), 7.49 (d, 1H, Ar–H, J=8.7 Hz), 7.82 (d, 1H, Ar–H, J=8.7 Hz). ^{13}C NMR ($CDCl_3$): δ 14.11, 22.67, 26.01, 26.07, 29.10, 29.25, 29.35, 31.82, 68.25, 68.29, 96.22, 101.65, 103.88, 107.96, 113.19, 118.63, 127.77, 133.73, 149.88, 157.52, 160.07, 162.31, 163.30. Anal. Calcd for $C_{29}H_{41}NO_4$: C, 74.48; H, 8.84; N, 3.00. Found C, 74.45; H, 8.84; N, 2.93.

*4.1.9. 5-Dodecyloxy-2-(6-dodecyloxybenzoxazol-2-yl)phenol (**2a**; n=12).* White solid; yield 75%. ^{1}H NMR ($CDCl_3$): δ 0.86 (t, 6H, $-CH_3$, J=6.9 Hz), 1.25–1.46 (m, 36H, $-CH_2$), 1.73–1.84 (m, 4H, $-OCH_2CH_2$), 3.95–4.00 (m, 4H, $-OCH_2$), 6.51–6.58 (m, 2H, Ar–H), 6.91 (q, 1H, Ar–H, J=2.4 Hz), 7.06 (d, 1H, Ar–H, J=2.1 Hz), 7.50 (d, 1H, Ar–H, J=8.7 Hz), 7.82 (d, 1H, Ar–H, J=8.7 Hz). ^{13}C NMR ($CDCl_3$): δ 14.13, 22.70, 26.00, 26.05, 29.09, 29.24, 29.37, 29.60, 29.65, 31.93, 68.25, 68.93, 96.23, 101.66, 103.88, 107.98, 113.21, 118.64, 127.77, 133.73, 149.88, 157.52, 160.07, 162.31, 163.31. Anal. Calcd for $C_{37}H_{57}NO_4$: C, 76.64; H, 9.91; N, 2.42. Found C, 76.59; H, 9.92; N, 2.26.

*4.1.10. 5-Tetradecyloxy-2-(6-tetradecyloxybenzoxazol-2-yl)phenol (**2a**; n=14).* White solid. ^{1}H NMR ($CDCl_3$): δ 0.86 (t, 6H, $-CH_2$, J=6.9 Hz), 1.24–1.46 (m, 44H, $-CH_2$), 1.73–1.85 (m, 4H, $-OCH_2CH_2$), 3.97–4.01 (m, 4H, $-OCH_2$), 6.52–6.58 (m, 2H, Ar–H), 6.91 (q, 1H, Ar–H, J=2.4 Hz), 7.07 (d, 1H, Ar–H, J=1.8 Hz), 7.50 (d, 1H, Ar–H, J=8.7 Hz), 7.83 (d, 1H, Ar–H, J=8.7 Hz). ^{13}C NMR ($CDCl_3$): δ 14.13, 22.70, 26.00, 26.06, 29.10, 29.24, 29.38, 29.60, 29.68, 31.93, 68.25, 68.93, 96.23, 101.66, 103.88, 107.98, 113.20, 118.64, 127.77, 133.73, 149.88, 157.52, 160.07, 162.31, 163.30. Anal. Calcd for $C_{41}H_{65}NO_4$: C, 77.43; H, 10.30; N, 2.20. Found C, 77.24; H, 10.30; N, 2.08.

*4.1.11. 1-Hexadecyloxy-2-(6-hexadecyloxybenzoxazol-2-yl)phenol (**2a**; n=16).* White solid. ^{1}H NMR ($CDCl_3$): δ 0.84 (t, 6H, $-CH_3$, J=7.2 Hz), 1.22–1.46 (m, 52H, $-CH_2$), 1.72–1.83 (m, 4H, $-OCH_2CH_2$), 3.95–3.99 (m, 4H, $-OCH_2$), 6.50–6.57 (m, 2H, Ar–H), 6.90 (q, 1H, Ar–H, J=2.1 Hz), 7.06 (d, 1H, Ar–H, J=1.2 Hz), 7.49 (d, 1H, Ar–H, J=8.70 Hz), 7.82 (d, 1H, Ar–H, J=8.70 Hz). ^{13}C NMR ($CDCl_3$): δ 14.13, 22.70, 26.00, 26.05, 29.09, 29.24, 29.38, 29.60, 29.70, 31.93, 68.25, 68.93, 96.24, 101.66, 103.89, 107.98, 113.21, 118.65, 127.77, 133.75, 149.89, 157.52, 160.07, 162.31, 163.30. Anal. Calcd for $C_{45}H_{73}NO_4$: C, 78.10; H, 10.63; N, 2.02. Found C, 78.16; H, 10.59; N, 1.86.

*4.1.12. 2,3-Didodecyloxy-6-(6-dodecyloxybenzoxazol-2-yl)phenol (**2b**; n=12).* The solution of 2-hydroxy-4-dodecyloxy-*N*-(2-hydroxy-3, 4-didodecyloxybenzylidene)aniline (1.0 g, 1.31 mmol) dissolved in warm $CHCl_3$ was slowly added lead acetate $Pb(OAc)_4$ (0.69 g, 1.57 mmol), and the solution was gently refluxed for 4 h. The solution was filtered off and the solution was extracted twice with CH_2Cl_2/H_2O. The organic layers were combined and dried over $MgSO_4$. The product was purified by flash chromatography (silica gel) eluting with hexane/CH_2Cl_2 (5/1). The product isolated as white solids was obtained by recrystallization from CH_2Cl_2/CH_3OH. Yield 80%. ^{1}H NMR ($CDCl_3$): δ 0.86 (t, 9H, $-CH_3$, J=6.8 Hz), 1.25–1.50 (m, 54H, $-CH_2$), 1.77–1.83 (m, 6H, $-OCH_2$), 3.99 (t, 2H, $-OCH_2$, J=6.5 Hz), 4.02–4.06 (m, 4H, $-OCH_2$), 6.55 (d, 1H, Ar–H, J=8.9 Hz), 6.91 (dd, 1H, Ar–H, J=2.2 Hz), 6.93 (dd, 1H, Ar–H, J=2.23 Hz), 7.07(s, 1H, Ar–H), 7.51 (d, 1H, Ar–H, J=8.7 Hz), 7.62 (d, 1H, Ar–H, J=8.8 Hz). ^{13}C NMR ($CDCl_3$): δ 14.11, 22.69, 26.05, 26.09, 29.12, 29.23, 29.30, 29.35, 29.38, 29.41, 29.53, 29.59, 29.64, 29.66, 29.70, 29.73, 30.28, 31.93, 68.95, 73.38, 96.23, 104.83, 105.47, 113.28, 118.81, 121.77, 133.71, 136.49, 149.93, 152.90, 156.25, 157.63, 162.23. IR (neat): 2917, 2850, 1651, 1505, 1457, 1295, 1237, 1117, 1082 cm^{-1}. MS (FAB): calcd for MH^+ $C_{49}H_{82}NO_5$: 764.6. Found: 764.2.

*4.1.13. 2,3-Dioctyloxy-6-(6-octyloxybenzoxazol-2-yl)phenol (**2b**; n=8).* White solid; yield 75%. ^{1}H NMR ($CDCl_3$): δ 0.85 (t, 9H, $-CH_3$, J=6.8 Hz), 1.25–1.47 (m, 30H, $-CH_2$), 1.73–1.86 (m, 6H, $-OCH_2$), 3.95–4.08 (m, 6H, $-OCH_2$), 6.55 (d, 1H, Ar–H, J=8.8 Hz), 6.89 (dd, 1H, Ar–H, J=2.3 Hz), 6.94 (dd, 1H, Ar–H, J=2.3 Hz), 7.06 (s, 1H, Ar–H), 7.51 (d, 1H, Ar–H, J=8.7 Hz), 7.62 (d, 1H, Ar–H, J=8.8 Hz). ^{13}C NMR ($CDCl_3$): δ 14.11, 22.68, 26.03, 29.28, 29.35, 29.58, 29.65, 30.25, 31.82, 31.87, 68.88, 73.35, 96.15, 104.71, 105.42, 113.22, 118.78, 121.75, 133.67,

136.38, 149.89, 152.85, 156.20, 157.58, 162.19. IR (neat): 3088, 2917, 2850, 1632, 1503, 1462, 1295, 1235, 1104, 1082 cm^{-1}. MS (FAB): calcd for MH^+ $C_{37}H_{57}NO_5$: 596.4. Found: 596.0.

*4.1.14. 2,3-Didecyloxy-6-(6-decyloxybenzoxazol-2-yl)phenol (**2b**; n=10).* White solid; yield 85%. ^1H NMR ($CDCl_3$): δ 0.85–0.88 (m, 9H, $-CH_3$), 1.24–1.50 (m, 42H, $-CH_2$), 1.78–1.82 (m, 6H, $-OCH_2$), 3.99 (t, 2H, $-OCH_2$, J=6.5 Hz), 4.02–4.06 (m, 4H, $-OCH_2$), 6.55 (d, 1H, Ar–H, J=8.9 Hz), 6.91 (dd, 1H, Ar–H, J=2.2 Hz), 6.92 (dd, 1H, Ar–H, J=2.2 Hz), 7.06 (s, 1H, Ar–H), 7.51 (d, 1H, Ar–H, J=8.7 Hz), 7.62 (d, 1H, Ar–H, J=8.8 Hz). ^{13}C NMR ($CDCl_3$): δ 14.11, 22.69, 26.05, 26.09, 29.24, 29.42, 29.57, 29.58, 29.65, 29.70, 30.28, 31.92, 31.94, 68.94, 73.37, 96.22, 104.82, 105.47, 113.27, 118.81, 121.76, 133.72, 136.49, 149.93, 152.91, 156.24, 157.63, 162.23. IR (neat): 2917, 2850, 1632, 1503, 1466, 1295, 1237, 1117, 1080 cm^{-1}. MS (FAB): calcd for MH^+ $C_{43}H_{70}NO_5$: 680.5. Found: 680.1.

*4.1.15. 2,3-Ditetradecyloxy-6-(6-tetradecyloxybenzooxazol-2-yl)phenol (**2b**; n=14).* White solid; yield 87%. ^1H NMR ($CDCl_3$): δ 0.86 (t, 9H, $-CH_3$, J=6.9 Hz), 1.24–1.49 (m, 66H, $-CH_2$), 1.78–1.83 (m, 6H, $-OCH_2$), 3.99 (t, 2H, $-OCH_2$, J=6.6 Hz), 4.02–4.06 (m, 4H, $-OCH_2$), 6.55 (d, 1H, Ar–H, J=8.9 Hz), 6.91 (dd, 1H, Ar–H, J=2.2 Hz), 6.93 (dd, 1H, Ar–H, J=2.2 Hz), 7.07 (s, 1H, Ar–H), 7.51 (d, 1H, Ar–H, J=8.7 Hz), 7.62 (d, 1H, Ar–H, J=8.9 Hz). ^{13}C NMR ($CDCl_3$): δ 14.12, 22.70, 26.05, 26.09, 29.24, 29.31, 29.38, 29.40, 29.42, 29.59, 29.67, 29.68, 29.71, 29.74, 30.28, 31.94, 68.94, 73.37, 96.22, 104.82, 105.47, 113.27, 118.81, 121.76, 133.72, 136.49, 149.93, 152.90, 156.24, 157.63, 162.23. IR (neat): 2913, 2848, 1634, 1505, 1470, 1293, 1237, 1111, 1082 cm^{-1}. MS (FAB): calcd for MH^+ $C_{55}H_{94}NO_5$: 848.7. Found: 848.2.

*4.1.16. 2,3-Dihexadecyloxy-6-(6-hexadecyloxybenzooxazol-2-yl)phenol (**2b**; n=16).* White solid; yield 82%. ^1H NMR ($CDCl_3$): δ 0.86 (t, 9H, $-CH_3$, J=6.9 Hz), 1.24–1.49 (m, 78H, $-CH_2$), 1.79–1.83 (m, 6H, $-OCH_2$), 3.99 (t, 2H, $-OCH_2$, J=6.6 Hz), 4.02–4.06 (m, 4H, $-OCH_2$), 6.55 (d, 1H, Ar–H, J=9.0 Hz), 6.91 (dd, 1H, Ar–H, J=2.3 Hz), 6.93 (dd, 1H, Ar–H, J=2.3 Hz), 7.07 (s, 1H, Ar–H), 7.51 (d, 1H, Ar–H, J=8.7 Hz), 7.62 (d, 1H, Ar–H, J=8.9 Hz). ^{13}C NMR ($CDCl_3$): δ 14.11, 22.70, 26.05, 26.09, 29.24, 29.31, 29.37, 29.40, 29.60, 29.65, 29.68, 29.71, 29.73, 30.28, 31.94, 68.95, 73.37, 96.22, 104.82, 105.48, 113.27, 118.81, 121.76, 133.73, 136.49, 149.93, 152.91, 156.25, 157.63, 162.24. IR (neat): 2917, 2850, 1638, 1501, 1468, 1300, 1273, 1115, 1082 cm^{-1}. MS (FAB): calcd for MH^+ $C_{61}H_{106}NO_5$: 932.8. Found: 932.3.

*4.1.17. 5-Chloro-2-(6-decyloxybenzoxazol-2-yl)phenol (**2c**; X=Cl).* ^1H NMR ($CDCl_3$): δ 0.86 (t, 3H, $-CH_3$, J=6.0 Hz), 1.26–1.47 (m, 14H, $-CH_2$), 1.76–1.85 (m, 2H, $-OCH_2CH_2$), 3.99 (t, 2H, $-OCH_2$, J=6.6 Hz), 6.95 (m, 2H, Ar–H), 7.10 (m, 2H, Ar–H), 7.55 (d, 1H, Ar–H, J=9.0 Hz), 7.85 (d, 1H, Ar–H, J=8.7 Hz). ^{13}C NMR ($CDCl_3$): δ 14.13, 22.70, 26.05, 29.20, 29.34, 29.40, 29.58, 31.91, 68.95, 96.14, 109.61, 113.88, 117.56,119.24, 120.10, 126.97, 127.51, 133.32, 138.52, 150.06, 158.19, 158.73, 161.18.

*4.1.18. 2-(6-Decyloxybenzoxazol-2-yl)-5-methoxyphenol (**2c**; X=OCH_3).* ^1H NMR ($CDCl_3$): δ 0.86 (t, 3H, $-CH_3$, J=6.3 Hz), 1.26–1.46 (m, 14H, $-CH_2$), 1.75–1.85 (m, 2H, $-OCH_2CH_2$), 3.83 (s, 3H, $-OCH_2$), 3.98 (t, 2H, $-OCH_2$, J=6.6 Hz), 6.55 (d, 1H, Ar–H, J=8.7 Hz), 6.60 (s, 1H, Ar–H), 6.91(d, 1H, Ar–H, J=8.7 Hz), 7.07(s, 1H, Ar–H), 7.51 (d, 1H, Ar–H, J=9.0 Hz), 7.84 (d, 1H, Ar–H, J=8.4 Hz). ^{13}C NMR ($CDCl_3$): δ 14.13, 22.69, 26.06, 29.23, 29.34, 29.41, 29.58, 31.91,55.49, 68.94, 96.25, 101.19, 104.09, 107.57, 113.30, 118.67, 127.86, 149.89, 157.59, 160.14, 162.23, 163.74, 183.86.

*4.1.19. 2-(6-Decyloxybenzoxazol-2-yl)-5-fluorophenol (**2c**; X=F).* ^1H NMR ($CDCl_3$): δ 0.86 (t, 3H, $-CH_3$, J=6.6 Hz), 1.26–1.46 (m, 14H, $-CH_2$), 1.75–1.85 (m, 2H, $-OCH_2CH_2$), 3.98 (t, 2H, $-OCH_2$, J=6.6 Hz), 6.81–6.96 (m, 2H, Ar–H), 7.10(d, 1H, Ar–H, J=7.5 Hz), 7.69 (d, 1H, Ar–H, J=8.7 Hz), 8.07 (t, 1H, Ar–H, J=7.8 Hz). ^{13}C NMR ($CDCl_3$): δ 14.13, 22.69, 26.05, 29.21, 29.34, 29.40, 29.58, 31.91, 68.95, 96.18,104.31, 104.64, 107.32, 107.63, 113.71, 119.10, 128.26, 128.41, 133.29, 149.98, 158.02, 159.99, 160.17, 161.36, 163.94, 167.27.

*4.1.20. Bis[5-decyloxy-2-(6-decyloxybenzooxazol-2-yl)phenol]Pd(II) (**1a**–**Pd**; n=12).* The solution of 5-decyloxy-2-(6-decyloxybenzooxazol-2-yl)phenol (0.15 g, 0.28 mmol) dissolved in 30 mL of warm dry C_2H_5OH/THF (10:1) and palladium(II) acetate (33 mg, 0.147 mmol) dissolved in 10 mL dry C_2H_5OH was mixed. The solution was gently refluxed for 4 h. The dark brown solids were collected, and the product isolated as yellow solids was obtained after recrystallization from THF/CH_3OH. Yield 61–65%.

Anal. Calcd for **1a** (n=8) $C_{58}H_{80}N_2O_8Pd$: C, 67.00; H, 7.76; N, 2.69. Found C, 67.18; H, 7.95; N, 2.73.

Anal. Calcd for **1a** (n=10) $C_{66}H_{96}N_2O_8Pd$: C, 68.82; H, 8.40; N, 2.43. Found C, 69.15; H, 8.50; N, 2.50.

Anal. Calcd for **1a** (n=12) $C_{74}H_{112}N_2O_8Pd$: C, 70.31; H, 8.93; N, 2.22. Found C, 70.07; H, 8.95; N, 2.26.

Anal. Calcd for **1a** (n=14) $C_{82}H_{128}N_2O_8Pd$: C, 71.56; H, 9.37; N, 2.04. Found C, 71.71; H, 9.35; N, 2.02.

Anal. Calcd for **1a** (n=16) $C_{90}H_{144}N_2O_8Pd$: C, 72.62; H, 9.75; N, 1.88. Found C, 72.58; H, 9.80; N, 1.95.

*4.1.21. Bis[5-decyloxy-2-(6-decyloxybenzoxazol-2-yl)phenol]Cu(II) (**1a**–**Cu**; n=12).* The solution of 5-decyloxy-2-(6-decyloxybenzooxazol-2-yl)phenol (0.20 g, 0.34 mmol) dissolved in 30 mL of warm dry C_2H_5OH/THF (10:1) and copper(II) acetate (36 mg, 0.18 mmol) dissolved in 10 mL dry C_2H_5OH was mixed. The solution was gently refluxed for 4 h. The dark brown solids were collected, and the product isolated as brown solids was obtained after recrystallization from THF/CH_3OH. Yield 68–75%. Anal. Calcd for **1b** (n=12) $C_{74}H_{112}N_2O_8Cu$: C, 72.78; H, 9.24; N, 2.29. Found C, 72.87; H, 9.26; N, 2.26.

*4.1.22. Bis[5-decyloxy-2-(6-decyloxybenzoxazol-2-yl)phenol]Zn(II) (**1a**–**Zn**; n=12).* The solution of 5-decyloxy-2-(6-decyloxybenzooxazol-2-yl)phenol (0.15 g, 0.28 mmol) dissolved in 30 mL of warm dry C_2H_5OH/THF (10:1) and zinc(II) acetate (30 mg, 0.145 mmol) dissolved in 10 mL dry C_2H_5OH was mixed. The solution was gently refluxed for 4 h. The off-white solids were collected, and the product isolated as white solids was obtained after recrystallization from THF/CH_3OH. Yield 65–77%. Anal. Calcd for $C_{74}H_{112}N_2O_8Zn$: C, 72.67; H, 9.23; N, 2.29. Found C, 72.4; H, 9.27; N, 2.24.

*4.1.23. Bis[2,3-didodecyloxy-6-(6-dodecyloxybenzoxazol-2-yl)phenol]zinc(II) (**1b**–**Zn**, n=12).* The solution of 2,3-didodecyloxy-6-(6-dodecyloxybenzooxazol-2-yl)phenol (0.2 g, 0.26 mmol) dissolved in 5.0 mL of dried THF was slowly added a solution of zinc(II) acetate (34.0 mg, 0.16 mmol) dissolved in 3.0 mL of absolute C_2H_5OH/THF (10/1). The mixture was refluxed for 20 h. Brown solids were collected, and the product isolated as a light yellow as obtained after recrystallization from THF/CH_3OH. Yield 85%. MS (FAB): calcd for $C_{98}H_{161}N_2O_{10}Zn$: 1589.1. Found: 1589.0 $[M+H]^+$. Anal. Calcd for $C_{98}H_{160}N_2O_{10}Zn$: C, 73.95; H, 10.13; N, 1.76. Found: C, 73.83; H, 10.17; N, 1.70.

Compound **1b**–**Zn** (n=8) Anal. Calcd for $C_{74}H_{112}N_2O_{10}Zn$: C, 70.81; H, 8.99; N, 2.23. Found: C, 70.23; H, 10.07; N, 2.29.

Compound **1b**–**Zn** (n=10) Anal. Calcd for $C_{86}H1_{136}N_{98}O_{10}Zn$: C, 72.57; H, 9.63; N, 1.97. Found: C, 72.26; H, 9.87; N, 1.76.

Compound **1b**–**Zn** (n=14) Anal. Calcd for $C_{110}H_{184}N_2O_{10}Zn$: C, 75.06; H, 10.54; N, 1.59. Found: C, 75.23; H, 10.65; N, 2.12.

Compound **1b**–**Zn** (n=16) Anal. Calcd for $C_{122}H_{208}N_2O_{10}Zn$: C, 75.99; H, 10.87; N, 1.45. Found: C, 75.92; H, 10.03; N, 1.25.

*4.1.24. Bis[2,3-didecyloxy-6-(6-decyloxybenzoxazol-2-yl)phenol]copper(II) (**1b**–**Cu**, n=10).* The procedures were similar to above Zn complex (**1a**) except that copper(II) acetate hydrate was used. Yield 80%. Anal. Calcd for $C_{98}H_{160}N_2O_{10}Cu$: C, 74.03; H, 10.10; N, 1.76. Found: C, 74.17; H, 10.16; N, 1.79.

*4.1.25. Bis[2,3-didodecyloxy-6-(6-dodecyloxybenzoxazol-2-yl)phenol]palladium(II) (**1b**–**Pd**, n=10).* The procedures were similar to above Zn complex (**1a**) except that palladium(II) acetate was used. Yield 75%. Anal. Calcd for $C_{86}H_{136}N_2O_{10}Pd$: C, 70.53; H, 9.36; N, 1.91. Found: C, 70.07; H, 9.30; N, 1.90.

Acknowledgements

We thank the National Science Council of Taiwan, ROC (NSC 98-2113-M-008-003-MY2) in generous support of this work.

Supplementary data

Supplementary data associated with this article can be found in the online version at doi:10.1016/j.tet.2011.07.024.

References and notes

1. (a) Porta, B.; Jamal Khamsi, J.; Noveron, J. C. *Curr. Org. Chem.* **2008**, *12*, 1–24; (b) *Liquid Crystals II; Structure and Bonding*; Donnio, B., Bruce, D. W., Eds.; Spring: Berlin Heidelberg, 1999; Vol. 95, pp 193–247; (c) *Inorganic Materials*; Bruce, D. W., Ed.; John Wiley: New York, NY, 1997; (d) *Metallomesogens: Synthesis, Properties, and Applications*; Serrano, J. L., Ed.; VCH: Weiheim, 1996.
2. (a) Venkataramanan, N. S.; Kuppuraj, G.; Rajagopal, S. *Coord. Chem. Rev.* **2005**, *249*, 1249–1268; (b) Cozzi, P. G. *Chem. Soc. Rev.* **2004**, *33*, 410–421.
3. (a) Basova, T.; Latteyer, F.; Atilla, D.; Gürek, A. G.; Hassan, A.; Ahsen, V.; Peisert, H.; Chassè, T. *Thin Solid Films* **2010**, *518*, 5745–5752; (b) Zharnikova, N.; Usol'tseva, N.; Kudrik, E.; Thelakkat, M. *J. Mater. Chem.* **2009**, *19*, 3161–3167; (c) de la Escosura, A.; Martínez-Díaz, M. V.; Barbera, J.; Torres, T. *J. Org. Chem.* **2008**, *73*, 1475–1480; (d) Kimura, M.; Ueki, H.; Ohta, K.; Shirai, H.; Kobayashi, N. *Langmuri* **2006**, *23*, 5051–5056; (e) Makhseed, S.; Bumajdad, A.; Ghanem, B.; Msayi, K.; McKeown, N. B. *Tetrahedron Lett.* **2004**, *45*, 4865–4868; (f) Yılmaz, F.; Atilla, D.; Ahsen, V. *Polyhedron* **2004**, *23*, 1931–1937; (g) Kimura, M.; Narikawa, H.; Ohta, K.; Hanabusa, K.; Shirai, H.; Kobayashi, N. *Chem. Mater.* **2002**, *14*, 2711–2717; (h) Cammidge, A. N.; Gopee, H. *Chem. Commun.* **2002**, 966–967; (i) Swarts, J. C.; Langner, E. H. G.; Krokeide-Hove, N.; Cook, M. J. *J. Mater. Chem.* **2001**, *11*, 434–443.
4. (a) Xiao, Z.-Y.; Hou, J.-L.; Jiang, X.-K.; Li, Z.-T.; Ma, Z. *Tetrahedron* **2009**, *65*, 10182–10191; (b) Shearman, G. C.; Yahioglu, G.; Kirstein, J.; Milgrom, L. R.; Seddon, J. M. *J. Mater. Chem.* **2009**, *19*, 598–604; (c) Tylleman, B.; Gomez-Aspe, R.; Gbabode, G.; Geerts, Y. H.; Sergeyev, S. *Tetrahedron* **2008**, *64*, 4155–4161; (d) Jin, L.-M.; Yin, J.-J.; Chen, L.; Zhou, J. M.; Xiao, J.-C.; Guo, C.-C.; Chen, Q.-Y. *Chem. Eur. J.* **2006**, *12*, 7935–7941; (e) Li, J.; Xin, H.; Li, M. *Liq. Cryst.* **2006**, *33*, 913–919; (f) Arunkumar, C.; Bhyrappa, P.; Varghese, B. *Tetrahedron Lett.* **2006**, *47*, 8033–8037; (g) Segade, A.; Lopez-Calahorra, F.; Velasco, D. *Mol. Cryst. Liq. Cryst.* **2005**, *439*, 201–208; (h) Segade, A.; Castella, M.; Lopez-Calahorra, F.; Velasco, D. *Chem. Mater.* **2005**, *17*, 5366–5374; (i) Liu, W.; Shi, Y.; Shi, T.; Liu, G.; Liu, Y.; Wang, C.; Zhang, W. *Liq. Cryst.* **2003**, *30*, 1255–1257; (j) Castella, M.; Lopez-Calahorra, F.; Velasco, D. *Liq. Cryst.* **2002**, *29*, 559–565.
5. Bykoval, V.; Usol'tseva1, N.; Kudrik, E.; Galanin, N.; Shaposhnikov, G.; Yakubov, L. *Mol. Cryst. Liq. Cryst.* **2008**, *494*, 38–47.
6. Stepien, M.; Donnio, B.; Sessler, J. L. *Chem.—Eur. J.* **2007**, *13*, 6853–6863.
7. (a) Singh, A. K.; Kumari, S.; Kumar, K. R.; Sridhar, B.; Rao, T. R. *Polyhedron* **2008**, *27*, 181–186; (b) Singh, A. K.; Kumari, S.; Kumar, K. R.; Sridhar, B.; Rao, T. R. *Polyhedron* **2008**, *27*, 1937–1941; (c) Aiello, I.; Bellusci, A.; Crispini, A.; Ghedini, M.; Pucci, D.; Spataro, D. *Mol. Cryst. Liq. Cryst.* **2008**, *481*, 1–13.
8. (a) Crispini1, A.; Ghedini, M.; Pucci, D. *Beilstein J. Org. Chem.* **2009**, *5*, 1–6; (b) Morale, F.; Date, R. W.; Guillon, D.; Bruce, D. W.; Finn, R. L.; Wilson, C.; Blake, A. J.; Schr̈der, M.; Donnio, B. *Chem.—Eur. J.* **2003**, *9*, 2484–2501; (c) Pucci, D.; Barberio, G.; Crispini, A.; Francescangeli, O.; Ghedini, M.; Deda, M. L. *Eur. J. Inorg. Chem.* **2003**, 3649–3661.
9. Seredyuk, M.; Gaspar, A. B.; Ksenofontov, K.; Reiman, S.; Galyametdinov, Y.; Haase, H.; Rentschler, E.; Gutlich, P. *Chem. Mater.* **2006**, *18*, 2513–2519.
10. Ovejero, P.; Mayoral, M. J.; Cano, M.; Campo, J. A.; Heras, J. V.; Fernandez-Tobar, P.; Valién, M.; Pinilla, E.; Torres, M. R. *Mol. Cryst. Liq. Cryst.* **2008**, *481*, 34–55.
11. Wilson, C. J.; James, L.; Mehl, G. H.; Boyle, R. W. *Chem. Commun.* **2008**, 4582–4584.
12. Lehmann, M.; Sierra, T.; Barbera, J.; Serrano, J. L.; Parkerb, R. *J. Mater. Chem.* **2002**, *12*, 1342–1350.
13. (a) Mori, A.; Mori, R.; Takemoto, M.; Yamamoto, S. I.; Kuribayashi, D.; Uno, K.; Kubo, K.; Ujiie, S. *J. Mater. Chem.* **2005**, *15*, 3005–3014; (b) Elliott, J. M.; Chipperfield, J. R.; Clark, S. *Inorg. Chem.* **2002**, *41*, 293–299.
14. Yagi, S.; Hamakubo, K.; Ikawa, S.; Nakazumi, H.; Mizutani, T. *Tetrahedron* **2008**, *64*, 10598–10604.
15. Lee, C. K.; Ling, M. J.; Lin, I. J. B. *Dalton Trans.* **2003**, 4731–4737.
16. (a) Terazzi, E.; Bénech, J. M.; Rivera, J. P.; Bernardinelli, G.; Donnio, B.; Guillon, D.; Piguet, C. *Dalton Trans.* **2003**, 769–772; (b) Terazzi, E.; Torelli, S.; Bernardinelli, G.; Rivera, J. P.; Bénech, J. M.; Bourgogne, C.; Donnio, B.; Guillon, D.; Imbert, D.; Bünzli, J. G.; Pinto, A.; Jeannerat, D.; Piguet, C. *J. Am. Chem. Soc.* **2005**, *127*, 888–903.
17. (a) Pucci, D.; Aiello, I.; Bellusci, A.; Crispini, A.; Ghedini, M.; Deda, M. L. *Eur. J. Inorg. Chem.* **2009**, 4274–4281; (b) Taylora, R. A.; Ellis, H. A. *Liq. Cryst.* **2009**, *36*, 257–268.
18. (a) Bhattacharjee, C. R.; Das, G.; Mondal, P.; Rao, N. V. S. *Polyhedron* **2010**, *29*, 3089–3096; (b) Morale, F.; Finn, R. L.; Collinson, S. R.; Blake, A. J.; Wilson, C.; Bruce, D. W.; Guillon, D.; Donnio, B.; Schroder, M. *New J. Chem.* **2008**, *32*, 297–305; (c) Cavero, E.; Uriel, S.; Romero, P.; Serrano, J. L.; Gimenez, R. *J. Am. Chem. Soc.* **2005**, *129*, 11608–11618; (d) Barberio, R.; Bellusci, A.; Crispini, A.; Ghedini, M.; Golemme, A.; Prus, P.; Pucci, D. *Eur. J. Inorg. Chem.* **2005**, 181–188; (e) Pate, B. D.; Choi, S. M.; Werner-Zwanziger, U.; Baxter, D. V.; Zaleski, J. M.; Chisholm, M. H. *Chem. Mater.* **2002**, *14*, 1930–1936.
19. (a) Albayrak, C.; Özkan, N.; Dag, O. *Langmuir* **2011**, *27*, 870–873; (b) Martin, J. D.; Keary, C. L.; Thornton, T. A.; Novotnak, M. P.; Knutson, J. W.; Folmer, J. C. *Nat. Mater.* **2006**, *5*, 271–275; (c) Donnio, B. *Curr. Opin. Colloid Interface Sci.* **2002**, *7*, 371–394.
20. (a) Bhattacharjee, C. R.; Das, G.; Mondal, P.; Prasad, S. R.; Rao, D. S. S. *Eur. J. Inorg. Chem.* **2011**, 1418–1424; (b) Binnemans, K. *J. Mater. Chem.* **2009**, *19*, 448–453; (c) Pucci, D.; Aiello, I.; Bellusci, A.; Crispini, A.; Ghedini, M.; Deda, M. K. *J. Inorg. Chem.* **2009**, 4274–4281; (d) Wilson, C. J.; James, L.; Mehl, G. H.; Boyle, R. W. *Chem. Commun.* **2008**, 4582–4584.
21. Gimeneza, R.; Oriola, L.; Pinolb, M.; Serrano, J. L.; Vinualesa, A. I.; Fisherc, T.; Stumpe, J. *Helv. Chim. Acta* **2006**, *9*, 304–319.
22. (a) Chu, Q.; Medvetz, D. A.; Panzner, M. J.; Pang, Y. *Dalton Trans.* **2010**, *39*, 5254–5259; (b) Costa, T. M. H.; Stefani, V.; Gallas, M. R.; Balzaretti, N. M.; Jornada, J. A. H. D. *J. Mater. Chem.* **2001**, *11*, 3377–3381.
23. Abou-Zied, O. K.; Jimenez, R.; Thompson, E. H. Z.; Millar, D. P.; Romesberg, F. E. *J. Phys. Chem. A* **2002**, *106*, 3665–3672.
24. (a) Chen, C.-J.; Wu, Y.-C.; Sheu, H.-S.; Lee, G.-H.; Lai, C. K. *Tetrahedron* **2011**, *67*, 114–124; (b) Tsai, H.-H. G.; Chou, L.-C.; Lin, S.-C.; Sheu, H.-S.; Lai, C. K. *Tetrahedron Lett.* **2009**, *50*, 1906–1910; (c) Liao, C.-C.; Wang, C.-S.; Sheu, H.-S.; Lai, C. K. *Tetrahedron* **2008**, *64* 7977–7985; (d) Wang, H.-C.; Wang, Y.-J.; Hu, H.-M.; Lee, G.-H.; Lai, C. K. *Tetrahedron* **2008**, *64*, 4939–4948; (e) Wang, C.-S.; Wang, I.-W.; Cheng, K.-L.; Lai, C. K. *Tetrahedron* **2008**, *62*, 9383–9392; (f) Lai, C. K.; Liu, H.-C.; Li, F.-J.; Cheng, K.-L.; Sheu, H.-S. *Liq. Cryst.* **2005**, *32*, 85–94.